Soret Effect on Oscillatory MHD Convective Flow through a Porous Medium in a Vertical Channel with Thermal Radiation and Heat Source/Sink

Reena Devi
Department of Mathematics, ABV G Degree College Bangana, District Una, Himachal Pradesh, India.

***Abstract*—In this investigation, Soret effect over an oscillatory MHD convective flow through a porous medium in a vertical channel in the presence of thermal radiation and heat source/sink is investigated. A uniform magnetic field is applied in the direction normal to the plates. Exact solution of the equations governing the flow is obtained. The resulting velocity, temperature and concentration distributions and rate of heat transfer (Nusselt number Nu), rate of mass transfer (Sherwood number Sh) in terms of amplitude and phase are shown graphically for different values of the parameters entering into the problem. The skin-friction coefficient in terms of amplitude and phase angle is calculated and displayed in tables showing the effects of various parameters on them.**

***Index Terms*—Soret effect; Oscillatory; MHD; Radiation; Heat source/sink; Porous medium**

I. INTRODUCTION

MHD convective flows have a great significance not only of their own interest but also for the application in the fields of stellar and planetary magnetospheres, aeronautics, chemical engineering and electronics. In view of these applications a number of investigations have been reported in the literature. Hydromagnetic free convection flow through porous medium between two parallel plates has been investigated by Raptis et al. [17]. Attia and Kotb [1] analyzed the MHD flow between two parallel plates with heat transfer.

Unsteady MHD convective heat transfer past a semi-infinite vertical porous plate with variable suction has been investigated by Kim [13]. Attia [2] investigated the effectiveness of variation in the physical variables on mhd steady flow between parallel plates with heat transfer. Effects of unsteady free convective MHD flow through a porous medium bounded by an infinite vertical porous plate have been studied by Ahmed [3].

II. NOMENCLATURE

$\vec{V}$: velocity vector
p: pressure
$\vec{B}$: magnetic induction vector
$\vec{j}$: current density
t^*: time variable
g: acceleration due to gravity
K^*: permeability of the porous medium
T^*: temperature
C_p: specific heat at constant pressure
K: thermal conductivity
Q: radiative heat flux
Q^*: heat source/sink
C^*: species concentration
D: molecular diffusivity
D_1: thermal diffusivity
T_0: constant mean temperature
C_0: constant mean concentration
U: mean axial velocity
Re: Reynolds number
M: Hartmann number
K: permeability parameter
Gr: Grashof number
Gm: modified Grashof number
S: heat source/sink parameter
N: radiation parameter
Sc: Schmidt number
Sr: Soret number

Greek Letters
ρ: density
μ: coefficient of viscosity
υ: kinematic viscosity
β: coefficient of thermal expansion
β_c: coefficient of volume expansion due to concentration
ω^*: frequency of oscillation
ω: frequency parameter
Superscripts
*: Dimensional quantities.

Radiative convective flows are encountered in countless industrial and environment processes for example heating and cooling chambers, fossil fuel combustion energy processes, astrophysical flows, and solar power technology and space vehicle re-entry. Radiation effects on flow past an impulsively started vertical infinite plate has been investigated by Das et al. [9]. Bakier [6] studied the thermal radiation effects on mixed convection from vertical surfaces in saturated porous media. Effect of radiation on non-Darcy free convection from a vertical cylinder embedded in a fluid-saturated porous medium with a temperature-dependent viscosity has been studied by El-Hakim and Rashad [10]. Muthucumaraswamy and Kulandaivel [16] investigated the radiation effects on moving vertical plate with variable temperature and uniform mass diffusion. An exact solution of an oscillatory free convective MHD flow in a rotating porous channel with radiative heat has been investigated by Singh and Garg [19].

The phenomenon of heat and mass transfer has been the object of extensive research due to its applications in science and technology. Such phenomenons are observed in buoyancy induced motions in the atmosphere, in bodies of water, quasi-solid bodies such as earth. In nature and industrial applications many transport processes exist where the transfer of heat and mass takes place simultaneously as a result of combined buoyancy effects of thermal diffusion and diffusion of chemical species. In addition, the phenomenon of heat and mass transfer is also encountered in chemical process industries such as food processing and polymer production. In light of the above applications, many researchers studied the effects of heat and mass transfer on magnetohydrodynamic free convection flow: some of them are Rahman and Sattar [18], Yih [21], Aboeldahab and Elbarbary [4], Kim [14]. In the above stated papers, the thermal-diffusion term was neglected from the concentration equation. But when heat and mass transfer occur simultaneously in a moving fluid. The relations between the fluxes and the driving potentials are of nature that is more intricate. The mass transfer due to the temperature gradients is called Soret or thermal-diffusion effect. In general, the Soret effect is of a smaller order of magnitude than the effects discussed by Fourier's and Fick's law and are often neglected in heat and mass transfer processes. However, exceptions are observed therein. The Soret effect, for instance, has been utilized for isotope separation, and in mixtures between gases with very light molecular weight (H_2, He) and of medium molecular weight (N_2, air). Thermophoretic force has been used in commercial precipitators for applications similar to electrostatic precipitators. It is exploited in the manufacturing of optical fiber in vapor deposition processes. It can be important as a transport mechanism in fouling. Thermophoresis has also been shown to have potential in facilitating drug discovery by allowing the detection of aptamer binding by comparison of the bound versus unbound motion of the target molecule. This approach has been termed microscale thermophoresis. Furthermore, thermophoresis has been demonstrated as a versatile technique for manipulating single biological macromolecules, such as genomic-length DNA, in micro- and nanochannels by means of light-induced local heating. Thermophoresis is one of the methods used to separate different polymer particles in field flow fractionation. Thermodiffusion along with molecular diffusion occurs in many engineering systems and in nature. Thermodiffusion has a great effect on the Concentration distribution in a multicomponent mixture. The variations of composition and temperature may either lessen or enhance the separation in mixtures. The thermodiffusion phenomenon also plays a major role in the hydrodynamic instability analysis in mixtures, investigations of mineral migration, the mass transport modelling in living matters, and composition variation studies in hydrocarbon reservoirs.

In view of the importance of this Soret effect, Jha and Singh [11] studied the free convection and mass transfer flow about an infinite vertical flat plate

moving impulsively in its own plane, taking into account the Soret effects. Kafoussias [15] studied the same problem in the case of MHD flow. Soret effects on free convection and mass transfer flow with constant heat flux has been investigated by Jha [12]. Al-Azab [5] has investigated unsteady mixed convection heat and mass transfer past an infinite porous plate with thermophoresis effect. Balasubrahman et al. [7] studied the Soret effect on mixed convective heat and mass transfer through a porous medium confined in a cylindrical annulus under a radial magnetic field in the presence of constant heat source/sink. Singh et al. [20] studied the effect of thermophoresis on hydromagnetic mixed convection and mass transfer flow past a vertical permeable plate with variable suction and thermal radiation.

The objective of the present paper is to analyse the effects of Soret, radiation as well as heat source/sink effect on oscillatory MHD convective and mass transfer flow through a porous medium in a vertical channel.

III. BASIC EQUATIONS

The equations governing the unsteady radiating MHD free convective heat and mass transfer flow of an incompressible, viscous and electrically conducting fluid in a vertical channel filled with porous medium by taking into account Soret effect are:

Equation of Continuity:

$$div\vec{V} = 0, \tag{1}$$

Momentum Equation:

$$\rho\left[\frac{\partial\vec{V}}{\partial t^*} + \left(\vec{V}.\nabla\right)\vec{V} = -\nabla p + \vec{j}\times\vec{B} + \mu\nabla^2\vec{V} - \frac{\mu}{K^*}\vec{V} + g\beta T^* + g\beta_c C^*\right], \tag{2}$$

Energy Equation:

$$\rho C_p\left[\frac{\partial T^*}{\partial t^*} + \left(\vec{V}.\nabla\right)T^*\right] = k\nabla^2 T^* + Q^* T^* - \nabla q, \tag{3}$$

Concentration Equation:

$$\frac{\partial C^*}{\partial t^*} + \left(\vec{V}.\nabla\right)C^* = D\nabla^2 C^* + D_1\nabla^2 T^*, \tag{4}$$

Gauss's Law of Magnetism:

$$div\vec{B} = 0, \tag{5}$$

where the variables and related section quantities are defined in the Nomenclature section.

IV. FORMULATION OF THE PROBLEM

Consider an oscillatory MHD mixed convective flow of a viscous, incompressible and electrically conducting fluid through a porous medium in a vertical channel. The plates of the channel are at distance 'd' apart. The x^*-axis is oriented vertically upwards along the centreline of the channel. The z^*-axis taken perpendicular to the plates of the channel. A uniform magnetic field B_0 is applied along z*-axis. Since the plates of the channel are of infinite extent, all the physical quantities depend only on z^* and t^*. The Schematic diagram of the problem is shown in Figure 1.

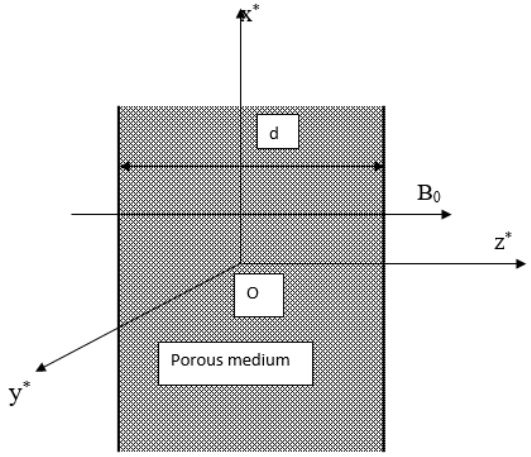

Figure 1. Schematic diagram of the Problem.

The equation of continuity (1) on integration gives $w^*=0$ where $\vec{V} = \left(u^*, v^*, w^*\right)$ be the velocity components in the direction $\left(x^*, y^*, z^*\right)$ respectively. A transverse magnetic field of uniform strength B_0 is applied along the z^*-axis.

Therefore, the equation (5) for the magnetic field $\vec{B} = \left(B_x^*, B_y^*, B_z^*\right)$ gives $B_z^* = B_0$ (constant).

Therefore, equations (2) to (4) reduces to

$$\frac{\partial u^*}{\partial t^*} = -\frac{1}{\rho}\frac{\partial p^*}{\partial x^*} + \upsilon\frac{\partial^2 u^*}{\partial z^{*2}} - \frac{\sigma B_0^2 u^*}{\rho} - \frac{\upsilon u^*}{K^*} + g\beta T^* + g\beta_c C^*, \tag{6}$$

$$\frac{\partial T^*}{\partial t^*} = \frac{k}{\rho C_p}\frac{\partial^2 T^*}{\partial z^{*2}} + Q^* T - \frac{\partial q}{\partial z^*}\,, \tag{7}$$

$$\frac{\partial C^*}{\partial t^*} = D\frac{\partial^2 C^*}{\partial z^{*2}} + D_1\frac{\partial^2 T^*}{\partial z^{*2}}, \tag{8}$$

The boundary conditions of the problem are:

$$u^* = T^* = C^* = 0 \text{ at } z^* = -\frac{d}{2}\,, \tag{9}$$

$$u^* = 0,\ T^* = T_0\cos\omega^* t^*\ ,\ C^* = C_0\cos\omega^* t^*\ ,$$

$$\text{at } z^* = \frac{d}{2}\ . \tag{10}$$

Following Cogley et al. (1968) the last term in the energy equation (7) stands for radiative heat flux is given by

$$\frac{\partial q}{\partial z^*} = 4\alpha^2 T^*, \tag{11}$$

where α is the mean radiation absorption coefficient.

We now introduce the following dimensionless variables:

$$\left.\begin{aligned} &\eta = \frac{z^*}{d}\ ,\ x = \frac{x^*}{d}\ ,\ y = \frac{y^*}{d}\ ,\ u = \frac{u^*}{U}\ ,\ v = \frac{v^*}{U}\\ &T = \frac{T^*}{T_0}\ \ ,\ \ C = \frac{C^*}{C_0}\ \ ,\ \ t = \frac{t^* U}{d}\ \ ,\ \ \omega = \frac{\omega^* d}{d} \end{aligned}\right\},$$

$$p = \frac{p^*}{\rho U^2}\ . \tag{12}$$

Then, introducing the relations (11) and (12) into the equations (6) to (8), respectively, we then obtain the following equations:

$$\frac{\partial u}{\partial t} = -\frac{\partial p}{\partial x} + \frac{1}{\mathrm{Re}}\frac{\partial^2 u}{\partial \eta^2} - \frac{M^2}{\mathrm{Re}}u - \frac{1}{K\,\mathrm{Re}}u + \frac{Gr}{\mathrm{Re}}T + \frac{Gm}{\mathrm{Re}}C, \tag{13}$$

$$\frac{\partial T}{\partial t} = \frac{1}{\mathrm{Pr}\,\mathrm{Re}}\frac{\partial^2 T}{\partial \eta^2} + \left(\frac{S}{\mathrm{Re}} - \frac{N^2}{\mathrm{Pr}\,\mathrm{Re}}\right)T, \tag{14}$$

$$\frac{\partial C}{\partial t} = \frac{1}{Sc\,\mathrm{Re}}\frac{\partial^2 C}{\partial \eta^2} + \frac{Sr}{\mathrm{Re}}\frac{\partial^2 T}{\partial \eta^2}, \tag{15}$$

Where $\mathrm{Re} = \frac{Ud}{\upsilon}$ is the Reynolds number, $M = Bd_0\sqrt{\frac{\sigma}{\rho\upsilon}}$ is the Hartmann number, $K = \frac{K^*}{d^2}$ is the permeability of the porous medium, $Gr = \frac{g\beta d^2 T_0}{\upsilon U}$ is the Grashof number, $Gm = \frac{g\beta_c d^2 C_0}{\upsilon U}$ is the modified Grashof number, $S = \frac{Q^* d^2}{\upsilon\rho C_p}$ is the heat source/sink parameter, $N = \frac{2\alpha d}{\sqrt{k}}$ is the radiation parameter, $Sc = \frac{\upsilon}{D}$ is the Schmidt number, $Sr = \frac{D_1 T_0}{\upsilon C_0}$ is the Soret number.

The corresponding boundary conditions are obtained as:

$$u = T = C = 0\,,\ \text{at } \eta = -\frac{1}{2}\ , \tag{16}$$

$$u = 0\,,\ T = \cos\omega t\,, C = \cos\omega t\ \ \text{, at } \eta = \frac{1}{2}\ . \tag{17}$$

For the oscillatory internal flow, we shall assume that the fluid flows under the influence of a non-dimensional oscillatory pressure gradient in the direction of x-axis which is of the form

$$-\frac{\partial p}{\partial x} = P\cos\omega t\cdot \tag{18}$$

V. METHOD OF SOLUTION

In order to solve the system of equations (13), (14) and (15) under the boundary conditions (16) and (17), we assume

$$u(\eta,t) = u_0(\eta)e^{\iota\omega t}\,, T(\eta,t) = \theta_0(\eta)e^{\iota\omega t}$$

$$, C(\eta,t) = C_0(\eta)e^{\iota\omega t}\ ,\ -\frac{\partial p}{\partial x} = Pe^{\iota\omega t}\,. \tag{19}$$

Substituting equation (19) into the equations (13) to (15), we get

$$\frac{d^2 u_0}{d\eta^2} - \left(M^2 + \frac{1}{K} + \iota\omega\,\mathrm{Re}\right)u_0 = -P\,\mathrm{Re} - Gr\theta_0 - GmC_0\,, \tag{20}$$

$$\frac{d^2\theta_0}{d\eta^2} - \left(N^2 + \iota\omega\,\mathrm{Pr}\,\mathrm{Re} - S\,\mathrm{Pr}\right)\theta_0 = 0\,, \tag{21}$$

$$\frac{d^2 C_0}{d\eta^2} - \iota Sc\,\mathrm{Re}\,\omega C_0 = -ScSr\frac{d^2\theta_0}{d\eta^2}, \tag{22}$$

The boundary conditions (16) and (17) reduces to

$$u_0 = \theta_0 = C_0 = 0\,,\ \text{at } \eta = -\frac{1}{2}\ , \tag{23}$$

$$u_0 = 0\,,\ \theta_0 = C_0 = 1\,,\ \text{at } \eta = \frac{1}{2}\ . \tag{24}$$

Substituting the solutions of equations (20) to (22) under the boundary conditions (23) and (24), we get

$$T(\eta,t)=\left[\frac{\sinh\left(\eta+\frac{1}{2}\right)a}{\sinh a}\right]e^{\iota\omega t}, \quad (25)$$

$$C(\eta,t)=\left\{\frac{\left[(1+ScSr)a^2-b^2\right]\sinh\left(\eta+\frac{1}{2}\right)b}{\left(a^2-b^2\right)\sinh b}-\frac{ScSra^2\sinh\left(\eta+\frac{1}{2}\right)a}{\left(a^2-b^2\right)\sinh a}\right\}e^{\iota\omega t}, \quad (26)$$

$$u(\eta,t)=\left\{\begin{array}{l}\frac{P\,\mathrm{Re}}{g^2}\left(1-\frac{\cosh g\eta}{\cosh\frac{g}{2}}\right)+\frac{Gr}{\left(a^2-g^2\right)}\left(\frac{\sinh\left(\eta+\frac{1}{2}\right)g}{\sinh g}-\frac{\sinh\left(\eta+\frac{1}{2}\right)a}{\sinh a}\right)\\ +\frac{Gm\left[(1+ScSr)a^2-b^2\right]}{\left(a^2-b^2\right)\left(b^2-g^2\right)}\left(\frac{\sinh\left(\eta+\frac{1}{2}\right)g}{\sinh g}-\frac{\sinh\left(\eta+\frac{1}{2}\right)b}{\sinh b}\right)\\ -\frac{GmScSra^2}{\left(a^2-b^2\right)\left(a^2-g^2\right)}\left(\frac{\sinh\left(\eta+\frac{1}{2}\right)g}{\sinh g}-\frac{\sinh\left(\eta+\frac{1}{2}\right)a}{\sinh a}\right)\end{array}\right\}e^{\iota\omega t}, \quad (27)$$

where $a^2=N^2+\iota\omega\,\mathrm{Pr}\,\mathrm{Re}-S\,\mathrm{Pr}$,

$b^2=\iota\omega Sc\,\mathrm{Re}$, $g^2=M^2+\frac{1}{K}+\iota\omega\,\mathrm{Re}$.

Skin-friction coefficient (τ_L) at the left plate, in terms of amplitude and phase, is:

$$\tau_L=\left(\frac{\partial u}{\partial\eta}\right)_{\eta=-\frac{1}{2}}=|F|\cos(\omega t+\alpha), \quad (28)$$

Heat transfer coefficient (Nu) at the left plate in terms of amplitude and phase

$$Nu=\left(\frac{\partial T}{\partial\eta}\right)_{\eta=-\frac{1}{2}}=|G|\cos(\omega t+\varphi), \quad (29)$$

Mass transfer coefficient (Sh) at the left plate in terms of amplitude and phase

$$Sh=\left(\frac{\partial C}{\partial\eta}\right)_{\eta=-\frac{1}{2}}=|H|\cos(\omega t+\gamma), \quad (30)$$

where $F=F_r+\iota F_i=\left(\frac{du_0}{d\eta}\right)_{\eta=-\frac{1}{2}}$

$$=\frac{P\,\mathrm{Re}}{g}\tanh\frac{g}{2}+\frac{Gr}{\left(a^2-g^2\right)}\left(\frac{g}{\sinh g}-\frac{a}{\sinh a}\right)+\frac{Gm\left[(1+ScSr)a^2-b^2\right]}{\left(a^2-b^2\right)\left(b^2-g^2\right)}\left(\frac{g}{\sinh g}-\frac{b}{\sinh b}\right)$$
$$-\frac{GmScSra^2}{\left(a^2-b^2\right)\left(a^2-g^2\right)}\left(\frac{g}{\sinh g}-\frac{a}{\sinh a}\right)$$

, $\alpha=\tan^{-1}\frac{F_i}{F_r}$, $G=G_r+\iota G_i=\left(\frac{d\theta_0}{d\eta}\right)_{\eta=-\frac{1}{2}}$

$=\frac{a}{\sinh a}$, $\varphi=\tan^{-1}\frac{G_i}{G_r}$,

$$H=H_r+\iota H_i=\left(\frac{dC_0}{d\eta}\right)_{\eta=-\frac{1}{2}}$$

$$=\frac{\left[(1+ScSr)a^2-b^2\right]b}{\left(a^2-b^2\right)\sinh b}-\frac{ScSra^2}{\left(a^2-b^2\right)\sinh a},$$

$\gamma=\tan^{-1}\frac{H_i}{H_r}$.

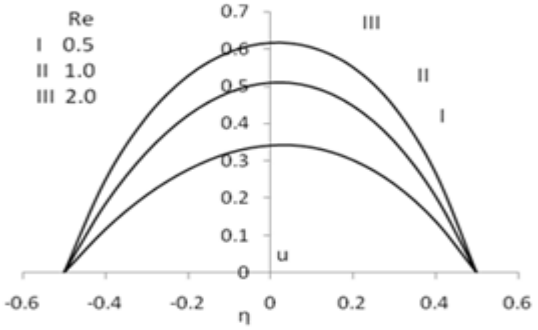

Figure 2. Variation of velocity profiles with Re for Gr=1, Gm=1, K=1, Pr=0.7, M=1, N=1, S=0.5, Sc=0.60, Sr=1, P=5, ω=5 and t=0.

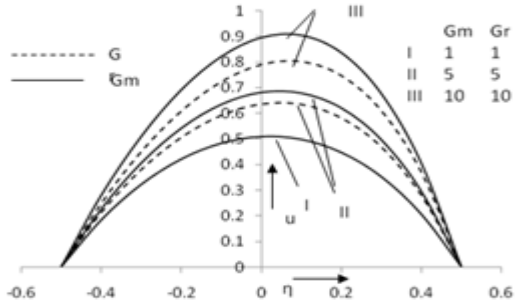

Figure 3. Variation of velocity profiles with Gm and Gr for Re=1, K=1, Pr=0.7, M=1, N=1, S=0.5, Sc=0.60, Sr=1, P=5, ω=5 and t=0.

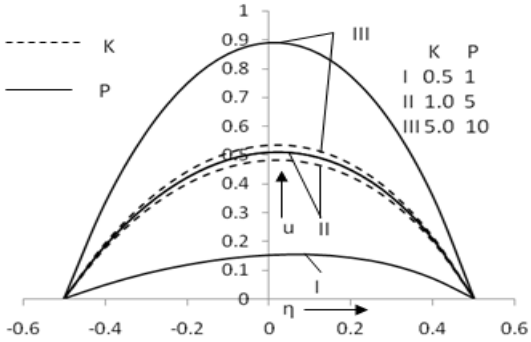

Figure 4. Variation of velocity profiles with K and Pfor Re=1, Gr=1, Gm=1, Pr=0.7, M=1, N=1, S=0.5, Sc=0.60, Sr=1, ω=5 and t=0.

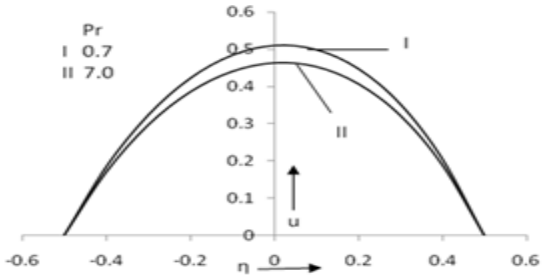

Figure 5. Variation of velocity profiles with Pr for Re=1, Gr=1, Gm=1, K=1, M=1, N=1, S=0.5, Sc=0.60, Sr=1, P=5, ω=5 and t=0.

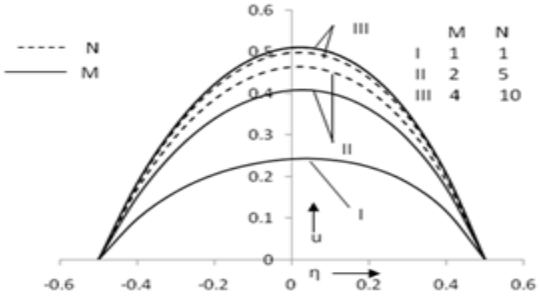

Figure 6. Variation of velocity profiles with M and N for Re=1, Gr=1, Gm=1, K=1, Pr=0.7, N=1, S=0.5, Sc=0.60, Sr=1, P=5, ω=5 and t=0.

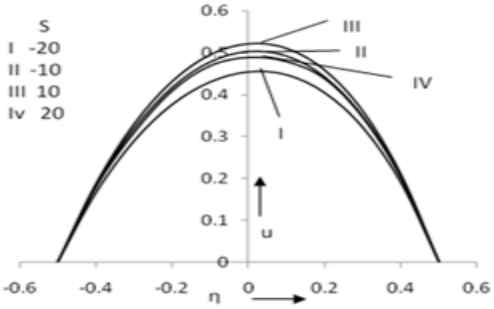

Figure 7. Variation of velocity profiles with S for Re=1, Gr=1, Gm=1, K=1, Pr=0.7, M=1, N=1, Sc=0.60, Sr=1, P=5, ω=5 and t=0.

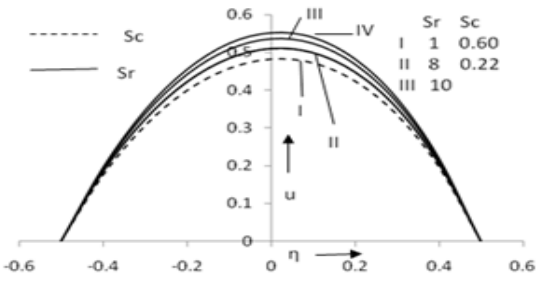

Figure 8. Variation of velocity profiles with Sr and Sc for Re=1, Gr=1, Gm=1, K=1, Pr=0.7, M=1, N=1, S=0.5, P=5, ω=5 and t=0.

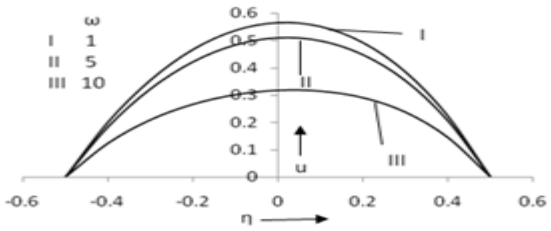

Figure 9. Variation of velocity profiles with ω for Re=1, Gr=1, Gm=1, K=1, Pr=0.7, M=1, N=1, S=0.5, Sc=0.60, Sr=1, P=5 and t=0.

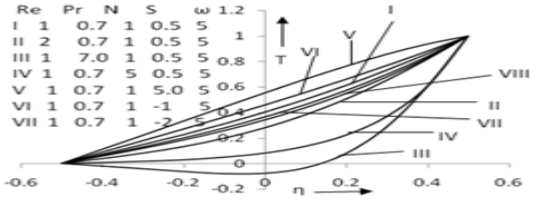

Figure 10. Variation of temperature profiles for t = 0.

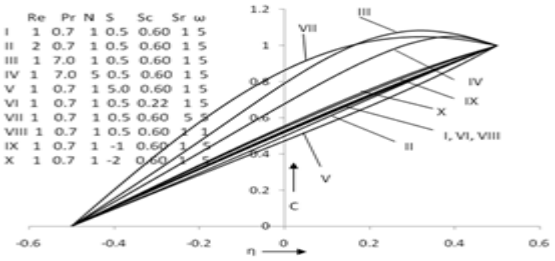

Figure 11. Variation of concentration profiles for t = 0.

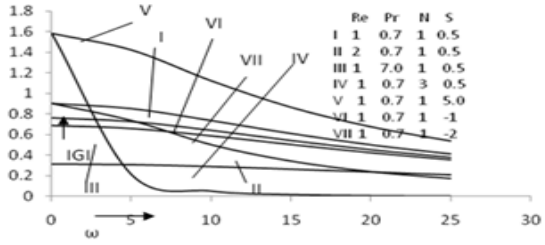

Figure 12. Amplitude $|G|$ of the rate of heat transfer.

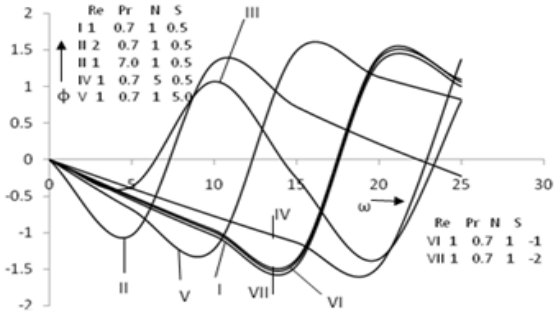

Figure 13. Phase angle φ of the rate of heat transfer.

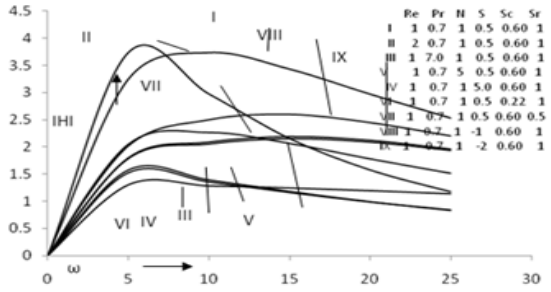

Figure 14. Amplitude $|H|$ of the rate of mass transfer.

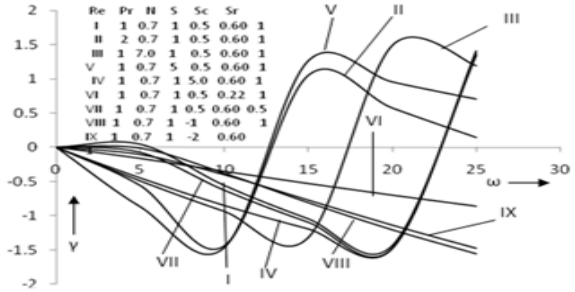

Figure 15. Phase angle γ of the rate of mass transfer.

Table 1: Amplitude $|F|$ of the skin-friction.

Re	Gr	Gm	K	Pr	M	N	S	Sc	Sr	P	ω = 0	ω = 5	ω = 10	ω = 15	ω = 20	ω = 25
1	1	1	1	0.7	1	1	0.5	0.60	1	5	1.618	2.219	1.819	1.46	1.201	1.025
2	1	1	1	0.7	1	1	0.5	0.60	1	5	3.771	3.502	2.397	1.844	1.557	1.385
1	5	1	1	0.7	1	1	0.5	0.60	1	5	2.117	2.614	2.025	1.522	1.182	.968
1	1	5	1	0.7	1	1	0.5	0.60	1	5	1.02	2.735	2.202	1.682	1.292	1.027
1	1	1	0.5	0.7	1	1	0.5	0.60	1	5	1.727	2.098	1.756	1.433	1.191	1.022
1	1	1	1	7.0	1	1	0.5	0.60	1	5	1.644	2.167	1.772	1.428	1.186	1.021
1	1	1	1	0.7	2	1	0.5	0.60	1	5	1.688	1.895	1.641	1.377	1.166	1.012
1	1	1	1	0.7	1	5	0.5	0.60	1	5	1.58	2.179	1.786	1.443	1.197	1.029
1	1	1	1	0.7	1	1	5	0.60	1	5	1.614	2.24	1.829	1.46	1.198	1.021
1	1	1	1	0.7	1	1	0.5	0.22	1	5	1.804	2.217	1.829	1.484	1.232	1.056
1	1	1	1	0.7	1	1	0.5	0.60	0.5	5	1.765	2.208	1.802	1.445	1.191	1.02
1	1	1	1	0.7	1	1	0.5	0.60	1	1	0.104	0.627	0.486	0.356	0.261	0.199
1	1	1	1	0.7	1	1	-1	0.60	1	5	1.613	2.213	1.816	1.46	1.202	1.026
1	1	1	1	0.7	1	1	-2	0.60	1	5	1.61	2.211	1.814	1.459	1.202	1.027

Table 2: Phase angle α of the skin-friction.

Re	Gr	Gm	K	Pr	M	N	S	Sc	Sr	P	ω = 0	ω = 5	ω = 10	ω = 15	ω = 20	ω = 25
1	1	1	1	0.7	1	1	0.5	0.60	1	5	0	-0.359	-0.613	-0.753	-0.814	-0.832
2	1	1	1	0.7	1	1	0.5	0.60	1	5	0	-0.575	-0.77	-0.8	-0.79	-0.777
1	5	1	1	0.7	1	1	0.5	0.60	1	5	0	-0.439	-0.745	-0.902	-0.952	-0.938
1	1	5	1	0.7	1	1	0.5	0.60	1	5	0	-0.411	-0.73	-0.927	-1.018	-1.035
1	1	1	0.5	0.7	1	1	0.5	0.60	1	5	0	-0.332	-0.575	-0.716	-0.783	-0.807
1	1	1	1	7.0	1	1	0.5	0.60	1	5	0	-0.363	-0.605	-0.734	-0.79	-0.807
1	1	1	1	0.7	2	1	0.5	0.60	1	5	0	-0.287	-0.51	-0.651	-0.725	-0.758
1	1	1	1	0.7	1	5	0.5	0.60	1	5	0	-0.356	-0.602	-0.735	-0.794	-0.814
1	1	1	1	0.7	1	1	5	0.60	1	5	0	-0.364	-0.622	-0.761	-0.821	-0.836
1	1	1	1	0.7	1	1	0.5	0.22	1	5	0	-0.352	-0.599	-0.738	-0.805	-0.832
1	1	1	1	0.7	1	1	0.5	0.60	0.5	5	0	-0.363	-0.614	-0.749	-0.806	-0.822
1	1	1	1	0.7	1	1	0.5	0.60	1	1	0	-0.472	-0.83	-1.048	-1.145	-1.149
1	1	1	1	0.7	1	1	-1	0.60	1	5	0	-0.358	-0.611	-0.75	-0.813	-0.831
1	1	1	1	0.7	1	1	-2	0.60	1	5	0	-0.358	-0.61	-0.749	-0.811	-0.83

VI. RESULTS

In order to understand physically the exact solution obtained we have evaluated the velocity field, temperature field, concentration field and skin-friction coefficient, rate of heat transfer (Nusselt number Nu), rate of mass transfer (Sherwood number Sh) in terms of amplitude and phase. The value of

Prandtl number Pr is taken to be 0.71 and 7.0 which corresponds to air and water respectively. The value of Schmidt number Sc is taken for Hydrogen (Sc=0.22) and water-vapour (Sc=0.60).

Figure 2 shows the variation of velocity profiles with Reynolds number Re. It is observed that velocity goes on increasing with the increase of Re. This is because inertial forces increase as we increase Reynolds number Re and these forces accelerates the fluid flow.

Figures 3, 4.6 and 8 are combined for two parameters and then one curve is common in each figure.

The variation of velocity profiles with Grashof number Gr and modified Grashof number Gm are exhibited in Figures 3. It is found from these Figures that velocity increases with the increase of Gr and Gm. The buoyancy force increases with the increase of Gr and Gm that lead to the increase in velocity. Figure 4 shows that velocity increases with the increase of permeability K of the porous matrix and with pressure gradient P. Figure 5 depicts the variation of velocity profiles with Prandtl number Pr. It is observed from this Figure that velocity decreases with the increase of Prandtl number Pr.

The variation of velocity profiles with Hartmann number M and with radiation parameter N is exhibited in Figure 6. It is observed that an increase in magnetic field has a retarding effect on the velocity field of the flow field. The presence of transverse magnetic field produces a resistive force on the fluid flow. This force is called the Lorentz force, which leads to slow down the motion of electrically conducting fluid. The increase of radiation parameter N leads to decrease in velocity.

The variation of velocity profiles with heat source/sink parameter S is presented in Figure 7. It is found from this Figure that velocity increases with the increase of S (<0) and decreases with the increase of S (>0) this implies that thermal source accelerates the fluid flow whereas thermal sink has reverse effect on it. Variation of velocity profiles with Schmidt number Sc and Soret number Sr is presented in Figure 8. These Figures shows that velocity increases with the increase of Sc and Sr.

It is clear from Figure 9 that the velocity decreases with the increase of frequency of oscillations ω.

Variation of temperature profiles with Reynolds number Re, Prandtl number Pr, radiation parameter N, heat source/sink parameter S and frequency of oscillations ω is presented in Figure 10. It is clear from this Figure that temperature increases with the increase of thermal source S(<0) and thermal sink S(>0) and decreases with the increase of Re, Pr, N and ω. Figure 11 depicts the variation of concentration profiles with Reynolds number Re, Prandtl number Pr, radiation parameter N, heat source/sink parameter S, Schmidt number Sc, Soret number Sr and frequency of oscillations ω. Figure shows that concentration decreases with the increase of Reynolds number Re, heat source/sink parameter S and increases with the increase of Pr, N, Sc and Sr and ω.

Amplitude $|G|$ of rate of heat transfer (Nusselt number Nu) is presented in Figure 12. It is observed from this Figure that amplitude $|G|$ increases with the increase of heat source/sink parameter S and decreases with the increase of Reynolds number Re, Prandtl number Pr and radiation parameter N. A decrease in $|G|$ is always noticed with the increasing frequency of oscillations ω. Phase angle β of rate of heat transfer (Nusselt number Nu) is presented in Figure 13. It is noticed that there is a phase lag initially for small values of the frequency of oscillation ω and thereafter the phase oscillates between phase lag and the phase lead. Amplitude $|H|$ of the rate of mass transfer (Sherwood number Sh) is depicted in Figure 14. Figure indicates that there is decrease in the amplitude $|H|$ with the increase of Pr nd N. However, H increases with the increase of Re, Sc and Sr. Also Figure 14 reveals that $|H|$ decreases with thermal sink S (>0) and increases with thermal source S (<0). The phase angle γ of the rate of mass transfer (Sherwood number Sh) is presented in Figure 15. It is noticed that there is a phase lag initially for small values of the frequency of oscillation ω and thereafter the phase oscillates between phase lag and the phase lead.

The skin-friction at the plate $\eta = -\frac{1}{2}$ is obtained in terms of its amplitude $|F|$ and the phase angle α. The amplitude $|F|$ is presented in Table I for different values of the parameters involved. The values in this table reveal that $|F|$ increases with Reynolds number Re, modified Grashof number Gm, permeability of

the porous medium K, pressure gradient P and Soret number Sr and decreases with increase of Prandtl number Pr, Hartmann number M, radiation parameter N, Schmidt number Sc. The amplitude $|F|$ increases for small ω but decreases for large ω with the increase of Grashof number Gr and heat source/sink parameter S. A decrease in $|F|$ is always noticed with the increasing frequency of oscillations ω. The phase angle α of the skin-friction is shown in Table II. The negative values in this table clearly indicate that there is always a phase lag. The phase lag α increases with Reynolds number Re, Grashof number Gr, modified Grashof number Gm, permeability of the porous medium K, heat source/sink parameter S, Schmidt number Sc and decreases with Prandtl number Pr, pressure gradient P, Hartmann number M, radiation parameter N and Soret number Sr.

VII. CONCLUSIONS

The velocity increases with the increase of Reynolds number Re, Grashof number Gr, modified Grashof number Gm, permeability of the porous medium K, thermal source S (<0), Schmidt number Sc, Soret number Sr and pressure gradient P. The increase in Prandtl number Pr, Hartmann number M, radiation parameter N, thermal sink S (>0) and frequency of oscillations ω leads to decrease in velocity.

Temperature increases with the increase of heat source/sink parameter S and decreases with the increase Re, Pr, N and ω. Concentration profiles increase with Pr, N, Sr, Sc and decreases with Re, heat source/sink parameter S and ω.

Amplitude $|G|$ of rate of heat transfer (Nusselt number Nu) increases with the increase of heat source/sink parameter S and decreases with the increase of Re, Pr and N.

Amplitude $|H|$ of the rate of mass transfer (Sherwood number Sh) decreases with the increase of Pr nd N and $|H|$ increases with the increase of Re, Sc and Sr. Also $|H|$ decreases with thermal sink S (>0) and increases with thermal source S (<0). For phase angle β of rate of heat transfer and phase angle γ of rate of mass transfer It is noticed that there is a phase lag initially for small values of ω and thereafter the phase oscillates between phase lag and the phase lead.

Amplitude $|F|$ of skin-friction increases with the increase of Re, Gm, K, P, Sr and decreases with increase of Pr, M, N, Sc. The amplitude $|F|$ increases for small ω but decreases for large ω with the increase of Grash of number Gr and heat source/sink parameter S.

For phase angle α of skin-friction there is always a phase lag.

REFERENCES

[1]. H. A. Attia and N. A. Kotb, "MHD flow between two parallel plates with heat transfer," *Acta Mechanica*, vol. 117, pp. 215–220, 1996.

[2]. H. A. Attia, "On the effectiveness of variation in the physical variables on the MHD steady flow between parallel plates with heat transfer," *International Journal for Numerical Methods in Engineering*, vol. 65, pp. 224–235, 2006.

[3]. A. Ahmed, "Effects of unsteady free convective MHD flow through a porous medium bounded by an infinite vertical porous plate," *Bulletin of the Calcutta Mathematical Society*, vol. 99, pp. 511–522, 2007.

[4]. E. M. Aboeldahab and E. M. E. Elbarbary, "Hall current effect on magnetohydrodynamic free convection flow past a semi-infinite vertical plate with mass transfer," *International Journal of Engineering Science*, vol. 39, pp. 1641–1652, 2001.

[5]. T. Al-Azab, "Unsteady mixed convection heat and mass transfer past an infinite porous plate with thermophoresis effect," *Transactions on Heat and Mass Transfer*, vol. 4, pp. 23–33, 2009.

[6]. A. Y. Bakier, "Thermal radiation effects on mixed convection from vertical surfaces in saturated porous media," *International Communications in Heat and Mass Transfer*, vol. 28, pp. 243–248, 2001.

[7]. M. Balasubrahmanyam, R. Sudarsan, and R. Siva Prasad, "Soret effect on mixed convective heat and mass transfer through a porous medium confined in a cylindrical annulus under a radial magnetic field in the presence of a constant heat source/sink," *IJAMM*, vol. 7, pp. 1–17, 2011.

[8]. A. C. Cogley, W. G. Vincent, and E. S. Giles, "Differential approximation for radiative

transfer in a non-gray near equilibrium," *American Institute of Aeronautics and Astronautics*, vol. 6, pp. 551–553, 1968.

[9]. U. N. Das, R. K. Deka, and V. M. Soundalgekar, "Radiation effects on flow past an impulsively started vertical infinite plate," *Journal of Theoretical Mechanics*, vol. 1, pp. 111–115, 1996.

[10]. M. A. El-Hakim and A. M. Rashad, "Effect of radiation on non-Darcy free convection from a vertical cylinder embedded in a fluid-saturated porous medium with a temperature-dependent viscosity," *Journal of Porous Media*, vol. 10, pp. 209–218, 2007.

[11]. B. K. Jha and A. K. Singh, "Soret effects on free convection and mass transfer flow in the Stokes problem for an infinite vertical plate," *Astrophysics and Space Science*, vol. 173, pp. 251–255, 1990.

[12]. B. K. Jha, "Soret effects on free convection and mass transfer flow with constant heat flux," *Modeling, Measurement and Control*, vol. 46, pp. 55–64, 1994.

[13]. Y. J. Kim, "Unsteady MHD convective heat transfer past semi-infinite vertical porous moving plate with variable suction," *International Journal of Engineering Science*, vol. 38, pp. 833–845, 2000.

[14]. Y. J. Kim, "Heat and mass transfer in MHD micropolar flow over a vertical moving porous plate in a porous medium," *Transport in Porous Media*, vol. 56, pp. 17–37, 2004.

[15]. N. G. Kafoussias, "MHD thermal-diffusion effects on free-convective and mass transfer flow over an infinite vertical moving plate," *Astrophysics and Space Science*, vol. 192, pp. 11–19, 1992.

[16]. R. Muthucumaraswamy and T. Kulandaivel, "Radiation effects on moving vertical plate with variable temperature and uniform mass diffusion," *Journal of Energy, Heat and Mass Transfer*, vol. 30, pp. 79–88, 2008.

[17]. A. Raptis, C. Massalas, and G. Tzivanids, "Hydromagnetic free convection flow through a porous medium between two parallel plates," *Physics Letters*, vol. 90, pp. 288–289, 1982.

[18]. M. M. Rahman and M. A. Sattar, "MHD free convection and mass transfer flow with oscillatory plate velocity and constant heat source in a rotating frame of reference," *Dhaka University Journal of Science*, vol. 49, pp. 63–73, 1999.

[19]. K. D. Singh and B. P. Garg, "Exact solution of an oscillatory free convection MHD flow in a rotating porous channel with radiative heat," *Proceedings of the National Academy of Sciences, India, Section A*, vol. 80, pp. 81–89, 2010.

[20]. N. P. Singh, A. K. Singh, A. K. Singh, and P. Agnihotri, "Effects of thermophoresis on hydromagnetic mixed convection and mass transfer flow past a vertical permeable plate with variable suction and thermal radiation," *Communications in Nonlinear Science and Numerical Simulation*, vol. 16, pp. 2519–2534, 2011.

[21]. K. A. Yih, "Free convection effect on MHD coupled heat and mass transfer of a moving permeable vertical surface," *International Communications in Heat and Mass Transfer*, vol. 26, pp. 95–104, 1999.